A Novel Antenna Array for GPS/INS/PL Integration

Mingquan Lu[1], Jinling Wang[2], Ravindra Babu[2], Dan Li[1] and Zhenming Feng[1]

[1]Department of Electronic Engineering, Tsinghua University, Beijing, P. R. China
Tel: +86-10-62792380, Fax: +86-10-62770317, Email: lumq@tsinghua.edu.cn

[2]School of Surveying & SIS, University of New South Wales, Sydney, Australia
Tel: +61 2 9385 4203, Fax: +61 2 9313 7493, Email: jinling.wang@unsw.edu.au

Abstract. In order to improve signal reception performance in GPS/INS/PL (Pseudolite) integration applications, a semi-sphere antenna array is proposed in this paper. It inherits the wide coverage characteristic of conventional spherical arrays and utilizes only about half the number of elements compared to a planar array to cover the upper-semi-sphere space above earth plane. It can process signals from both overhead and horizontal directions at the same time. Thus, unlike common planar arrays, this novel antenna array with a special geometry can receive satellite and Pseudolite (PL) signals from all directions, even from the horizon. Both Capon's and constraint methods have been used in the simulations of Direction of Arrival (DOA) estimation and beam-forming. These simulation results have demonstrated the advantages of the new array.

Key words: Antenna array, DOA, beamforming, semi-sphere, GPS/INS/PL.

1 Introduction

Due to its lower cost and good performance, GPS is considered as the primary source of navigation for many applications. However, GPS has its own limitations. A stand-alone GPS receiver can work well only if it can receive signals at least from 4 satellites with a reasonably good geometry. In addition, the GPS signal can also be jammed very easily by either intentional or unintentional interferences (Kaplan, 1996).

In order to get high positioning performance (e.g. accuracy and robustness), many multiple sensor integration schemes have been proposed, including GPS/GLONASS, GPS/INS, and GPS/INS/PL (Wang et al., 2001). Besides these integration methods, employing antenna arrays and adaptive filters can also substantially improve the GPS based positioning performance. An antenna array with a set of multi-channel receivers can significantly improve the position and location performance due to its anti-jamming and multipath mitigation property. As a result, the development of these spatial and temporal processing GPS receivers has become a hot topic in the research and industrial community (Amin et al 2003; Enge, 1999; Brown & Gerein, 2001).

Recently, several techniques based on antenna-array reception have been proposed (Malmström, 2003; Amin et al 2003). Among them, conventional planar antenna array is the most widely used in the researches (Brown & Gerein, 2001). However, the coverage of a general planar antenna array is limited in space. For example, these arrays cannot provide good reception performance if signals are received at low elevations. In fact, it is required to receive the satellite or Pseudolite signals at very low elevations in some environments. Obviously, employing a wide coverage antenna array with a GPS/INS/PL integrated system will be a good solution.

In order to overcome the limitations of the conventional planar antenna arrays, and improve signal reception performance in GPS, GPS/PL and GPS/INS/PL integrated applications, a semi-sphere antenna array is proposed in this paper. This array inherits the wide coverage characteristic of conventional spherical arrays and utilizes only about half the number of elements compared to a planar array to cover the upper-semi-spherical space above the earth plane. This property enhances the signal reception from both overhead and horizontal directions simultaneously. Thus, unlike common planar arrays, this novel antenna array with special geometry can receive satellite and Pseudolite signals from all directions, even from the horizon. Both Capon's and constraint methods have been used in the

simulations of Direction of Arrival (DOA) estimation and beam-forming. The simulation results have demonstrated the advantages of the new array.

The paper is organized as follows. Section II presents the array geometry and derives the received signal expressions.Section III gives two simulation examples to demonstrate the advantages of the array: one for DOA estimation, and the other for beam-forming. Section IV concludes the paper.

2 ANTENNA ARRAY ILLUSTRATION

2.1 Array Geometry

The geometry of the semi-sphere array is given in Figure 1. The array is assumed to have one element on the top with M circles where N elements are uniformly placed in each circle. Therefore, a total of $MN+1$ elements are distributed on the semi-spherical surface. The coordinates of each element in the (r, θ, ϕ) polar coordinate system can be expressed as:

$$\overrightarrow{r_{mn}} = (r_{mn}, \theta_{mn}, \phi_{mn}) = \begin{cases} (r, \theta_{mn}, \phi_{mn}), & 1 \leq m \leq M, 1 \leq n \leq N \\ (r, 0, \#), & m=0, n=0 \end{cases} \quad (1)$$

where r represents the radius of the sphere, the symbol ' # ' represents any real number, and $(r, 0, \#)$ is the coordinate of the element on the top of the semi-globe.

A far field source is assumed to be located at $\overrightarrow{r_s} = (r_s, \theta_s, \phi_s)$. For convenience, the centre of the bottom circle is selected as the phase reference point. Hence, every source impinging on the array will have a phase advance on each element relative to the reference point. The phase advance on $(m, n)_{th}$ element can be calculated with the following formulae:

$$\psi_{mns} = \frac{2\pi d_{mns}}{\lambda} \quad (2)$$

$$d_{mns} = r \frac{\overrightarrow{r_{mn}} \bullet \overrightarrow{r_s}}{r \cdot r_s} \quad (3)$$

where λ denotes the wavelength corresponding to the array working frequency, symbol ' $\bullet$ 'means inner product, and $\frac{\overrightarrow{r_{mn}} \bullet \overrightarrow{r_s}}{r \cdot r_s}$ is the cosine of the angle between the two vectors. In fact, $\vec{r} = (r, \theta, \phi)$ can also be denoted by Cartesian co-ordinates (x, y, z). A mapping between these two frames can be defined as

$$x = r \sin\theta \cos\phi, y = r \sin\theta \sin\phi, z = r \cos\theta \quad (4)$$

Thus, d_{mns} in equation (3) can be recalculated as

$$\begin{aligned} d_{mns} = & r(\sin\theta_{mn} \cos\phi_{mn} \sin\theta_s \cos\phi_s) \\ & + (\sin\theta_{mn} \sin\phi_{mn} \sin\theta_s \sin\phi_s) \\ & + (\cos\theta_{mn} \cos\theta_s) \end{aligned} \quad (5)$$

Specifically, $d_{00s} = r \cos\theta_s$. For almost all practical applications, equation (5) is normally used to calculate the phase advance.

2.2 Received Signals

With equations in section 2.1, the received signal on $(m, n)_{th}$ element can be expressed as

$$s_{mns} = f_{mn}(\theta_s, \phi_s) a_s e^{j\psi_s} e^{j\frac{2\pi}{\lambda} d_{mns}} \quad (6)$$

where $f_{mn}(\theta_s, \phi_s)$ is the pattern of $(m, n)_{th}$ element, $a_s e^{j\psi_s}$ represents the amplitude and phase characteristics of the impinging signal, and $f_{mn}(\theta_s, \phi_s) e^{j\frac{2\pi}{\lambda} d_{mns}}$ is the element of the so called steering vector, which can be written as

$$\begin{aligned} S(\theta_s, \phi_s) = & [f_{00}(\theta_s, \phi_s) e^{j\frac{2\pi}{\lambda} d_{00s}}, f_{11}(\theta_s, \phi_s) e^{j\frac{2\pi}{\lambda} d_{11s}}, \\ & ..., f_{mn}(\theta_s, \phi_s) e^{j\frac{2\pi}{\lambda} d_{mns}}, ..., f_{MN}(\theta_s, \phi_s) e^{j\frac{2\pi}{\lambda} d_{MNs}}]^T \end{aligned} \quad (7)$$

Generally, D far field uncorrelated signals are assumed to come from D different directions $\{(\theta_i, \phi_i), i = 1, \cdots, D\}$ with received power p_i. Noise on each element is uncorrelated, and white with zero mean and variance σ_n^2. The received signals on $(m, n)_{th}$ element is formulated as

$$x_{mn} = \sum_{i=1}^{D} s_{mni} + n_{mn} \quad (8)$$

where n_{mn} is the noise on $(m, n)_{th}$ element. The array received signal can be expressed as

$X = [x_{00}, x_{11}, \cdots, x_{mn}, \cdots, x_{MN}]^T$, which is a vector of length $MN+1$.

Now the covariance of the received signals at the entire array can be written as

$$R_{XX} = E[XX^H] \quad (9)$$

With some algebra manipulation, equation (9) can be reformulated as

$$R_{XX} = \sum_{i=1}^{D} p_i s_i s_i^H + \sigma_n^2 I \qquad (10)$$

where $s_i = [e^{j\psi_{00i}}, e^{j\psi_{11i}}, \cdots, e^{j\psi_{mni}}, \cdots, e^{j\psi_{MNi}}]^T$. Figure 1 is the illustration of the proposed semi-sphere antenna array geometry to receive a far field signal.
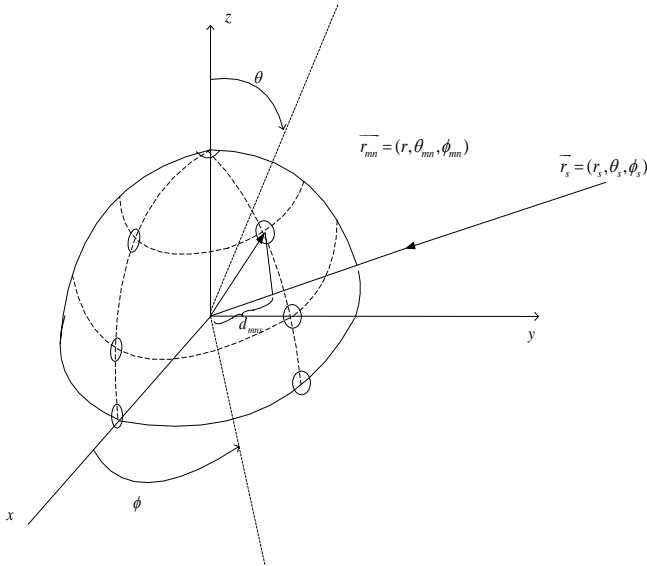
Figure 1. The proposed semi-sphere array

Figure 2. Single element pattern

3 SIMULATION RESULTS

In this section, a semi-sphere array with 19 elements (circles and elements per circle) is simulated. The projection of the element circles on the plane forms a concentric circle. The radius of the sphere is the wavelength of the L1 frequency (1575.42MHz) in free space. The difference between adjacent circles is the difference between adjacent elements in the same circle.

All the elements are assumed to have some pattern in their faced directions, where denotes the angle difference between the field and element position vectors. The single element pattern is shown in Figure 2, and the element patterns of the array are illustrated in Figure 3. For simulations, all signals and interferences are BPSK modulated, and assumed to be narrowband and uncorrelated with each other. Also, the space is defined in co-ordinates with units in degrees.
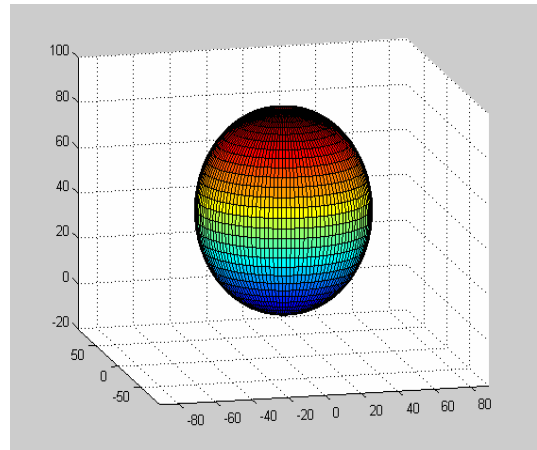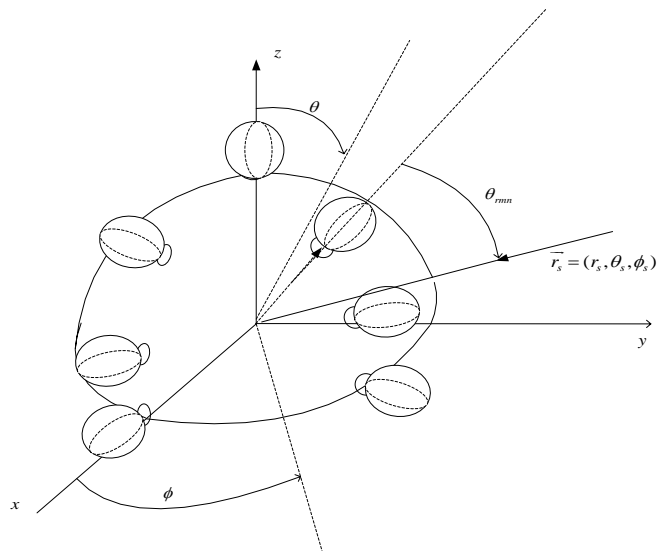
Figure 3. Element patterns of the array

3.1 DOA Estimation

In DOA estimation, 200 snapshots were taken and Capon's method (Capon, 1969) is employed to generate the spatial spectrum. The weights for calculating the spatial spectrum is obtained by

$$W_{\theta,\phi} = (R_{xx}^{-1} S_{\theta,\phi}) / (S_{\theta,\phi}^H R_{xx}^{-1} S_{\theta,\phi}) \qquad (11)$$

Various simulation experiments have been carried out to demonstrate the array's utilities. In Figure 4, 6 BPSK modulated signals clustered around vertex act as GPS signals with angles (5, 10), (15, 70), (10,130), (15,190), (10,250), (15,310), and a DOA 3D spectrum is plotted. SNRs are 20dB and 10dB for (a) and (b) respectively. The peaks representing the directions of the desired signals can be easily located when SNR is 20dB, while the peaks are hard to distinguish when SNR is 10dB.

From this figure, we also observe that the array can simultaneously locate 6 signals from the overhead.
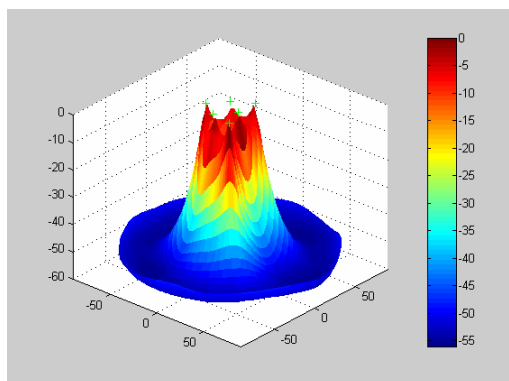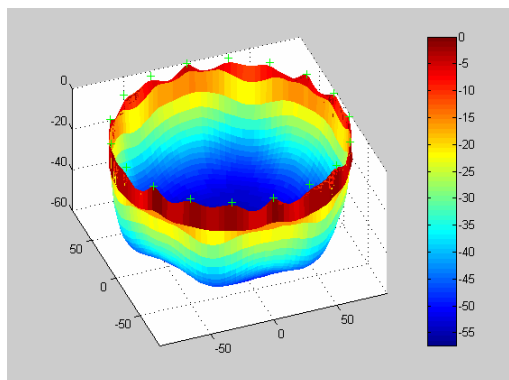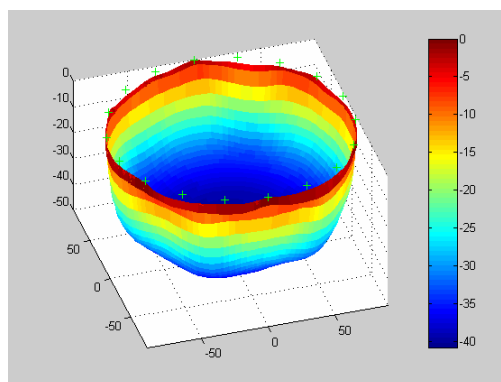

(a) SNR=INR=20dB
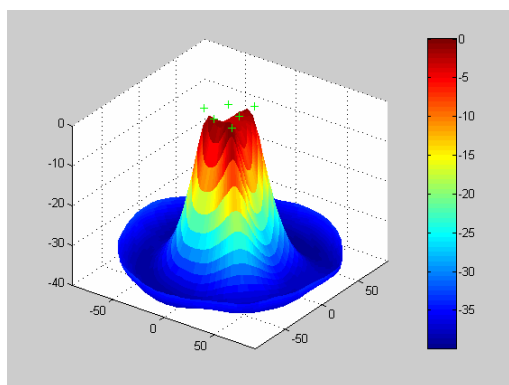
(b) SNR=INR=10dB

Figure 4. DOA spectrum for GPS signals with angles (5,10), (15,70), (10,130), (15,190), (10,250), (15,310).

In Figure 5, 18 BPSK modulated signals which simulate the Pseudolites are placed at the horizon at an angle (85,10), is uniformly distributed around the circle with 200 intervals, and a DOA 3D spectrum is plotted. In Figures 5 (a) and (b), SNR's are 20dB and 10dB respectively. The results show that 18 signals can be simultaneously located in horizon when the SNR's are high.
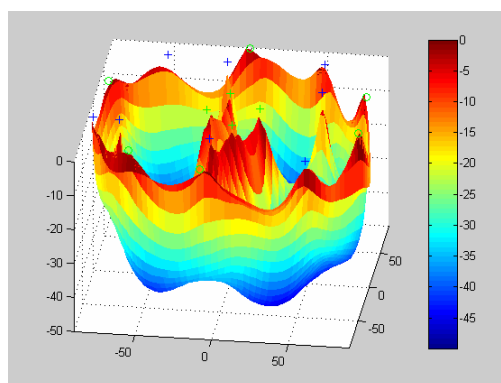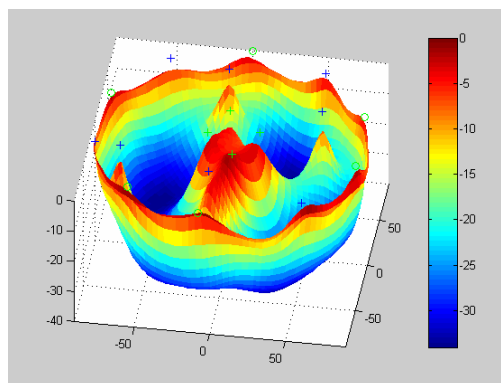

(a) SNR=INR=20dB

(b) SNR=INR=10dB

Figure 5. DOA spectrum for Pseudolite signals with directions (85,10), (85,30), (85,350).
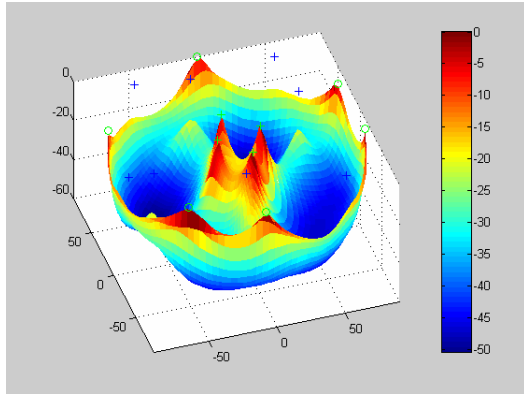

(a) SNR=INR=20dB

(b) SNR=INR=10dB

Figure 6. DOA spectrum for GPS, Pseudolite signals and interferences with angles (12, 10), (15,100), (10,190), (15,280), (82, 20), (87, 90), (84,160), (85,230), (87,265), (83,345), (30,260), (45, 30), (50,100), (55,200), (82, 55), (85,125), (87,195), (86,310).

In Figure 6, 4 BPSK modulated signals clustered around vertex act as GPS signals at angles (12,10), (15,100), (10,190), (15,280); 6 BPSK modulated signals from the horizon take the role of Pseudolite signals with angles (82,20), (87,90), (84,160), (85,230), (87,265), (83,345);8 BPSK modulated signals at angles (30,260), (45, 30), (50,100), (55,200), (82, 55), (85,125), (87,195), (86,310)

are considered as interferences. DOA 3D spectrum for SNR=20dB and SNR=10dB are respectively plotted in Figures 6 (a) and (b). From this figure, it can be observed that the array can simultaneously locate 18 signals.

The effect of the INR vibration on the DOA spectrum is shown in Figure 7. DOA's are the same as those in Figure 6; INR's are 10dB and 60dB respectively in Figures 7 (a) and (b), and SNR is 20dB in both subfigures.

(a) SNR=20dB, INR=10dB
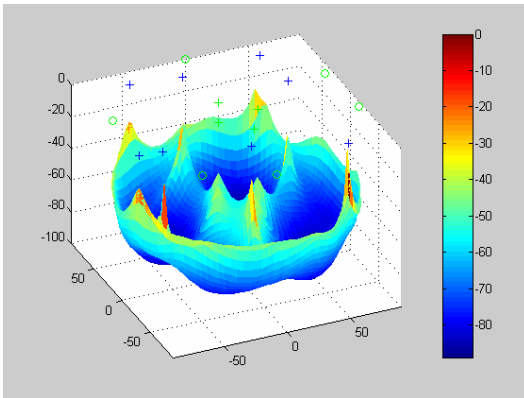
(b) SNR=20dB, INR=60dB

Figure 7. DOA spectrum for GPS, Pseudolite signals and interferences with angles (12, 10), (15,100), (10,190), (15,280), (82, 20), (87, 90), (84,160), (85,230), (87,265), (83,345), (30,260), (45, 30), (50,100), (55,200), (82, 55), (85,125), (87,195), (86,310)

3.2 Beam-forming

In beam-forming, DOA's are assumed to be known. A multiple constraint method can be employed to generate multiple beams for the desired signals and nulls at interferences by placing a unit response in the desired directions and zero response in undesired directions. Thus, the array weights can be obtained using the equation

$$W = C[C^H C]^{-1} f \tag{12}$$

where C, f are the signal steering vectors and corresponding constraints respectively; the equation

satisfies $C^H W = f$. For validations, the beam patterns of symmetrical signal distributions are simulated.

In Figure 8, 6 BPSK modulated signals clustered around vertex act as GPS/Pseudolite signals with angles (15, 10), (15, 70), (15,130), (15,190), (15,250), (15,310); 6 BPSK modulated signals from the horizon take the role of Pseudolite signals with angles (85, 10), (85, 70), (85,130), (85,190), (85,250), (85,310); 6 BPSK modulated signals at angles (45, 10), (45, 70), (45,130), (45,190), (45,250), (45,310) are considered as interferences; and a DOA 3D spectrum is plotted. From this figure, it can be concluded that the array is not very effective in receiving the signals from horizon.
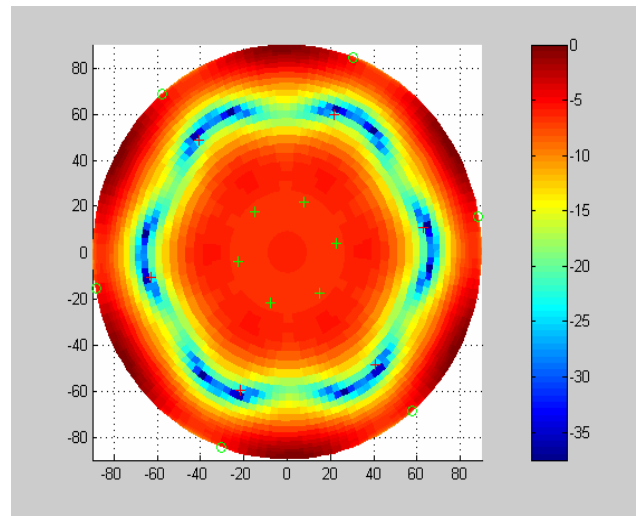

Figure 8. Beam pattern overview for GPS signals (15, 10), (15, 70), (15,130), (15,190), (15,250), (15,310). Pseudolite signals (85, 10), (85, 70), (85,130), (85,190), (85,250), (85,310) and interference (45, 10), (45, 70), (45,130), (45,190), (45,250), (45,310).
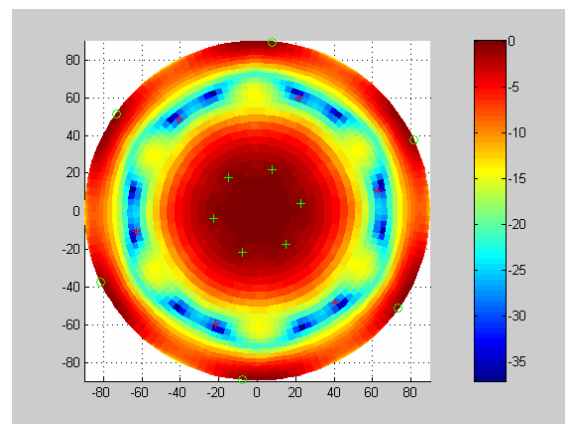

Figure 9. Beam pattern overview for GPS signals (15,10), (15,70), (15,130), (15,190), (15,250), (15,310), Pseudolite signals (85,25), (85,85), (85,145), (85,205), (85,265), (85,325) and interference (45,10), (45,70), (45,130), (45,190), (45,250), (45,310).

With GPS and interference signals direction fixed, the direction of Pseudolite signals are increased by 150, and the result is shown in Figure 9. It can be seen that both

signal reception and interference rejection have been improved.

With the GPS and Pseudolite signal directions fixed, the directions of interferences are decreased to 200, and the result is plotted in Figure 10. It can be seen that the horizontal signal reception becomes weaker.
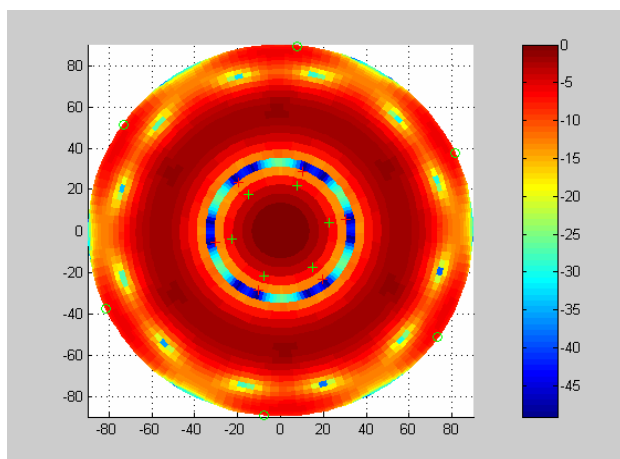

Figure 10. Beam pattern overview for GPS signals (15,10), (15, 70), (15,130), (15,190), (15,250), (15,310), Pseudolite signals (85,25), (85,85), (85,145), (85,205), (85,265), (85,325) and interference (20,10), (20,70), (20,130), (20,190), (20,250), (20,310).

4 Conclusions and outlook

In this paper, a semi-sphere array for GPS/INS/PL integration is proposed. The basic expressions are derived for this proposed new antenna array. The proposed semi-sphere antenna array can receive satellite and Pseudolite signals from all directions. Combined with adaptive processing, these semi-sphere antenna arrays based GPS, or GPS/PL, GPS/INS/PL integration receivers will possess strong anti-jamming capability. Therefore, this antenna array can be widely used in various applications to mitigate the multipath and interference signals, and also to receive low elevation Pseudolite signals. Simulation results on both the DOA estimation and

beam-forming demonstrated that the array can simultaneously process multiple signals from arbitrary directions in the upper semi-sphere. The power effect and spatial distribution effect of signals to the DOA spectrum and beam pattern were also analysed. This property of the semi-sphere antenna makes it very attractive in GPS based applications, including GPS/INS/PL integration.

References

Amin M.; Sun W.; and Lindsey A. (2003): *Adaptive arrays for GPS receivers*, in Ibnkahla M.Ed., Signal Processing for Mobile Communications Handbook, CRC Press.

Capon J. (1969): *High-resolution frequency-wave number spectrum analysis*, Proc. IEEE, 57:1408-1418.

Enge P. (1999): *Local area augmentation of GPS for the precision approach of aircraft*, Proc. IEEE, 87(1):111-132.

Kaplan ED. (1996): *Understanding GPS: Principles and Applications*, Artech House, Inc.

Wang J.; Dai L.; Tsuiji T.; Rizos C.; Grejner-Brzezinska D.; Toth C. (2001): *GPS/INS/Pseudolite Integration: Concepts, Simulation and Testing*. 14th Int. Tech. Meeting of the Satellite Division of the U.S. Inst. of Navigation, Salt Lake City, Ohio, 11-14 September, 2708-2715.

Malmström J. (2003): *Robust Navigation with GPS/INS and Adaptive Beamforming*, Scientific Report, FOI-R—0848—SE, Swedish Defence Research Agency, Sweden.

Brown A.; Gerein N. (2001): *Test Results of a Digital Beamforming GPS Receiver in a Jamming Environment*, ION GPS 2001, 11-14 September 2001, Salt Lake City, UT, 894-903.